Numerical Simulation of Cavitation around a Two-Dimensional Hydrofoil Using VOF Method and LES Turbulence Model

Ehsan Roohi **Amir Pouyan Zahiri**

Mahmud Pasandideh-Fard

Department of Mechanical Engineering, Ferdowsi University, Mashhad, Iran
P.O. Box 91775-1111

SUMMARY

In this paper simulation of cavitating flow over the Clark-Y hydrofoil is reported. This simulation is performed using the large eddy simulation (LES) turbulence model. To apply the cavitation model, the flow has been considered as a single fluid, two-phase mixture. A compressive volume of fluid (VOF) method is applied to track the interface of liquid and vapor phases. This simulation is performed using a finite volume, two phase solver available in the framework of the OpenFOAM package. Simulation is performed for the cloud cavitation regime. We compared the results of two different mass transfer models, namely Kunz and Sauer models. The results of our simulation are compared with the experimental data for cavitation dynamics, starting point of cavitation and force coefficients. Suitable accuracy has been observed.

Keywords: Clark-Y hydrofoil, cloud cavitation, LES, VOF, mass transfer model.

INTRODUCTION

Formation of vapor bubbles within a liquid when its pressure is less than the saturated vapor pressure is called cavitation. Cavitation usually could appear over marine vehicles such as marine propeller blades. The radial section of these marine blades is a two-dimensional hydrofoil [1]. Cavitation process is characterized by a dimensionless number; i.e., $\sigma = \frac{P_\infty - P_v}{0.5\rho U_\infty^2}$ called cavitation number, where P_v is the vapor pressure, ρ is the liquid density, and P_∞ and U_∞ are the free stream flow pressure and velocity, respectively.

Numerical simulation of cavitating flows had shown a rapid progress during the last two decades. The key challenges in numerical modeling of cavitating flows include sharp changes in the fluid density, existence of a moving boundary and the requirement of modeling phase change. Among different cavitation models, "homogeneous equilibrium flow model" had been widely employed [2]. Various categories in "homogeneous equilibrium flow model" differ in the relation that defines the variable density field. A barotropic water-vapor state law could be applied to evaluate density field. However, selection of an appropriate state law is a difficult task [3]. A more appropriate approach is to solve an advection equation for liquid or vapor volume fraction and compute density as a weighted average of the volume fraction of the two phases. This approach, namely "Transport Based Equation Model (TEM)", has extensively been used to simulate cavitating flows. Sauer [4] and Yuan et al. [5] suggested cavitation models based on the classical Rayleigh equation with some improvements. Singhal et al. [6], Merkle et al. [7] and Kunz et al. [8] suggested alternative mass transfer models based on semi-analytical equations. Senocak and Shyy [9] developed an analytical cavitation model based on the mass-momentum balance around the cavity interface.

Volume of Fluid (VOF) technique could be utilized to solve the advection equation of the volume fraction and predict the cavity interface accurately [10]. Different VOF methods for tracking free surface interface have been developed; i.e., SLIC [11], Hirt-Nichols [12], PLIC [13], and CICSAM [14-15]. In contrast to the geometric reconstruction algorithms [11-13], compressive scheme benefits from a high resolution differencing schemes to calculate volume fluxes [14]. Additionally, the implementation of compressive algorithms on arbitrary unstructured meshes is quite straightforward. VOF method can capture the cavity shape accurately. Frobenius and Schilling [16], Wiesche [17] and Bouziad et al. [18] used VOF technique to simulate cavitation over hydrofoils and pump impellers.

Since most of the cavitating flows perform at high Reynolds number and under unsteady condition, implementation of a suitable turbulence model in of great importance for accurate

Proceedings of the Eighth International Symposium on Cavitation (CAV 2012)
Edited by Claus-Dieter OHL, Evert KLASEBOER, Siew Wan OHL, Shi Wei GONG and Boo Cheong KHOO.

ISBN: 978-981-07-2826-7 :: doi:10.3850/978-981-07-2826-7_141

prediction of cavitation. Different approaches such asstandard or modified two-equation turbulence models have been utilized to implement turbulence effects on cavitating flows [19-23]. Use of "large eddy simulation (LES)" is another approach recently considered in numerical cavitation modelling [24-27].

As a continuation of our previous work [28], in this study we utilize a multi-phase flow solver of OpenFOAM package to simulate cloud cavitation regime over two-dimensional Clark-Y hydrofoil whose experimental data is available [2]. Our simulation employs a compressive VOF technique [15] which is combined with two mass transfer models, namely Sauer model [4] and Kunz et al. [8]. Moreover, in order to capture unsteady features of cavitating flow accurately, we use LES turbulence approach. PISO algorithm is used to solve the set of governing equations [29].The results of our simulation are compared with the experimental data for cavitation dynamics, starting point of cavitation and lift and drag coefficients.

2. Governing Equations

2.1 Implicit LES Model

Large eddy simulation (LES) is based on computing the large, energy-containing eddy structures which are resolved on the computational grid, whereas the smaller, more isotropic, sub grid structures are modeled. Development of the LES encounters a main obstacle of the strong coupling between sub grid scale (SGS) modeling and the truncation error of the numerical discretization scheme. This link could be exploited by developing discretization methods where the truncation error itself acts as an implicit SGS model. Therefore, the "implicit LES" expression is used to indicate approaches that merge SGS model and numerical discretization [30]. Furthermore, the cell-averaging discretisation of the flow variables can be thought of as an implicit filter. In the other words, finite volume discretization provides top-hat-shaped-kernel filtered values as:

$$\bar{f}_p = \frac{1}{(\delta V_p)} \int_{\Omega_p} f dV \tag{1}$$

, where over-bar denotes filtered quantity for cell Ω_p and V_p is the volume of the cell. Starting from the incompressible Navier-Stokes equations, the governing flow equations consisting of the balance equations of mass and momentum are:

$$\begin{aligned} &\partial_t(\rho v) + \nabla.(\rho v \times v) = -\nabla p + \nabla.s, \\ &\partial_t \rho + \nabla.(\rho v) = 0 \end{aligned} \tag{2}$$

, where v is the velocity, p is the pressure, $s = 2\mu D$ is the viscous stress tensor, where the rate-of-strain tensor is expressed as $D = \frac{1}{2}\left(\nabla v + \nabla v^T\right)$ and μ is the viscosity. The LES equations are theoretically derived, following Sagaut [31] from Eq. (2) by applying a low-pass filtering G = G(x, Δ), using a pre-defined filter kernel function such that,

$$\begin{aligned} &\partial_t(\rho \bar{v}) + \nabla.(\rho \bar{v} \times \bar{v}) = -\nabla \bar{p} + \nabla.(\bar{s} - B), \\ &\partial_t \rho + \nabla.(\rho \bar{v}) = 0 \end{aligned} \tag{3}$$

As no explicit filtering is employed, commutation errors in the momentum equation have been neglected. Equation (3) introduces one new term when compared to the unfiltered Eq. (2), i.e., the unresolved transport term B, which is the sub grid stress tensor. B can be decomposed as [32]:

$$B = \rho.\left(\overline{\bar{v} \times \bar{v}} - \bar{\bar{v}} \times \bar{\bar{v}} + \widetilde{B}\right) \tag{4}$$

, Where now only $\widetilde{B}$ needs to be modeled. The most common sub grid modeling approaches utilizes an eddy or sub grid viscosity, ν_{SGS}, similar to the turbulent viscosity approach in RANS, where ν_{SGS} can be computed in a wide variety of methods [32]. In the current study, sub grid scale terms are modeled using "one equation eddy viscosity" model available in the framework of OpenFOAM.

2.2 Multiphase Flow Modeling

To model cavitating flows, the two phases of liquid and vapor need to be specified as well as the phase transition mechanism between them. In this work, we consider a "two-phase mixture" method, which uses a local vapor volume fraction transport equation together with source terms for the mass transfer rate between the two phases due to cavitation.

$$\partial_t \gamma + \nabla.(\gamma \bar{v}) = \dot{m} \tag{5}$$

The density and viscosity in Eq. 5 are assumed to vary linearly with the vapor fraction,

$$\mu = \gamma \mu_v + (1-\gamma)\mu_l, \tag{6}$$

$$\rho = \gamma \rho_v + (1-\gamma)\rho_l. \tag{7}$$

In this work, we had employed both of Sauer and Kunz models. The approach chosen by Sauer [4] is given by:

$$\dot{m} = -\rho_v (1-\gamma)\frac{3\gamma}{R_b} sign(\bar{p} - p_v)\sqrt{\frac{2}{3}\frac{|\bar{p} - p_v|}{\rho_l}} \tag{8}$$

Sauer model expresses the vapor fraction as a function of the radius of the bubbles, R_b, which is assumed to be the same for all the bubbles. Kunz et al. [5] proposed a semi-analytical model as follows:

$$\frac{\partial \gamma}{\partial t} + \vec{\nabla} \cdot (\gamma \bar{v}) = \frac{C_{dest}\rho_v Min(P_l - P_v, 0)\gamma}{\rho_l (0.5\rho_l V_\infty^2) t_\infty} + \frac{C_{prod}(1-\gamma)\gamma^2}{\rho_l t_\infty} \tag{9}$$

, where C_{dest} and C_{prod} are two empirical constants. The main difference between the Eqs. (11-12) is in the condensation term which significantly affects the flow near the cavity closure region. Due to condensation, there will be a continuous flow of reentrant liquid jet near the cavity closure which in turn causes small vapor structures to detach from the end of the cavity continuously. To include this phenomenon more effectively, Kunz's model assumes a moderate rate of constant condensation. According to Senocak and Shyy [9], Kunz's model reconstructs the cavity region quite accurately especially in the closure region.

2.3 VOF Model

OpenFOAM uses an improved version of "The Compressive Interface Capturing Scheme for Arbitrary Meshes (CICSAM)"VOF technique, based on Ubbink's work [14]. CICSAM is implemented in OpenFOAM as an explicit scheme and could produce an interface that is almost as sharp as the geometric reconstruction schemes such as PLIC [13]. In CICSAM approach, a supplementary "interface-compression velocity (U_c)" is defined in the vicinity of the interface in such a way that the local flow steepens the gradient of the volume fraction function and the interface resolution is improved. This is incorporated in the conservation equation for volume fraction (γ) in the following form [33-34]:

$$\frac{\partial \gamma}{\partial t} + \nabla.(\gamma \bar{v}) + \nabla.[\bar{v}_c \gamma(1-\gamma)] = 0 \qquad (10)$$

The last term on the left-hand side of the above equation is known as the artificial compression term and it is non-zero only at the interface. The *compression* term stands for the role to shrink the phase-inter phase towards a sharper one [34]. The compression term does not bias the solution in any way and only introduces the flow of γ in the direction normal to the interface. In order to ensure this procedure, Weller [35] suggested the compression velocity to be calculated as:

$$\bar{v}_c = \min[C_\gamma |\bar{v}|, \max(|\bar{v}|)] \frac{\nabla \gamma}{|\nabla \gamma|} \qquad (11)$$

In other words, the compression velocity is based on the maximum velocity at the interface. The limitation of $\boldsymbol{v}_c$ is achieved through applying the largest value of the velocity in the domain as the worst possible case [35]. The intensity of the compression is controlled by a constant C_γ, i.e., it yields no compression if it is zero, a conservative compression for C_γ=1 and high compression for $C_\gamma > 1$ [34]. Nevertheless, the CICSAM algorithm is far less costly to apply compared to PLIC. Previous studies showed that OpenFOAM will give accurate results for the interface position on moderate to high resolution meshes [33-34]. The surface tension is evaluated per unit volume using the CSF model [36].

3. Results and Discussions

3.1 Simulation Set-up

The computational domain and boundary conditions are given according to the experimental setup described in Ref. [2] and are illustrated in Fig 1. The Clark-Y hydrofoil is placed at the center of the water tunnel with the angle of attack equal to 8 degree. The two important non-dimensional numbers used are the Reynolds number (Re) and cavitation number σ. The properties of the inlet free stream are used in these numbers defined. With the chord length equal to 7 cm, we have σ=0.8 and Re=7×10^5. Time step is set small enough so that the Courant number is less than 0.45 in the domain.

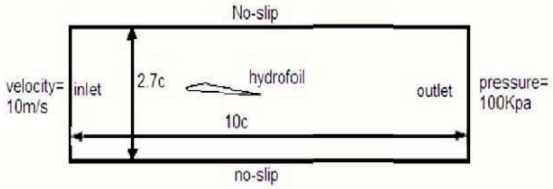

Figure 1: Computational domain and boundary conditions.

3.2 Grid Independency Study

As the Clark-Y hydrofoil is not geometrically complex, we used structured quadrilateral meshes. Mesh size near the wall has a key effect on the cavitation dynamics. Meshes are refined in both axial and normal directions to get a cavitation dynamic like the experimental data. The effect of using four different grid sizes on the average pressure profile, over one period of cavitation, on the upper and lower surfaces of the hydro foils shown in Fig. 2. Grids 1 to 4 have 65,130, 270 and 420 cells on the upper surface and 43, 87, 180 and 280 cells on the lower surface of the hydrofoil, respectively. It is observed that the difference between the pressure curves becomes negligible as the number of surface cells increases. Additionally, this figure shows that the grids 3 and 4 provide close solutions, especially for the upper surface where the cavitation occurs. Therefore, we performed our simulations using grid 3.

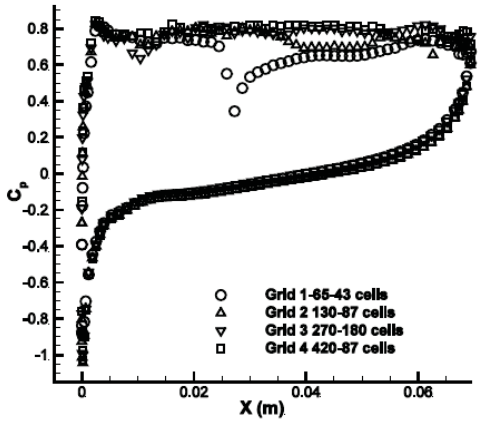

Figure 2: Investigating the effect of different grid sizes on the average pressure profile over the hydrofoil surfaces.

3.3 Cloud Cavitation Regime (σ=0.8)

At the first step, we consider the details of cloud cavitation regime over Clark-Y hydrofoil at σ=0.8. In this regime, some specific features including vapor cloud shedding at the end of cavity occurs. Therefore, a critical task of suitable turbulence model is to capture correct dynamics of cavity growth and detachment. We selected Clark-Y hydrofoil because experimental set of data is available in the literature [2].

Figure 3 shows density distribution (averaged in one period) over the upper surface of the hydrofoil obtained from two cavitation model, namely Kunz model and Sauer models. The coefficients of Kunz model are set as: $C_{dest} = 2.0\times10^4$, $C_{prod} = 1.0\times10^3$ [30]. Density is computed

from Eq. (7). As observed, Kunz model predicts that cavitation starts a bit ahead in comparison with Sauer model, to be more precise, Kunz model predicts that cavitation starts at x=10 mm, while Sauer model gives a value of x=14.4 mm. However, experimental data of Ref. [2] gives a value of x=9.8 mm. Therefore, Kunz model is more accurate. As cavity extends along the hydrofoil, both models predict an increase in the density field. Figure 5 shows average pressure coefficient distribution over the upper and lower surfaces of the cavity at σ=0.8. It is observed that both models predict close C_p distribution expect some deviations predicted in the Sauer model solution. On the upper surface, C_p=-σ near the leading edge but it slightly decreases as the flow approaches the trailing edge of the hydrofoil due to cavity detachments.

Figure 4 presents variation of lift coefficient on one cavitation cycle from two cavitation models in addition to experimental data reported in Ref. [22]. Due to changes in cavity length and cavity detachment (cloud shedding), lift forces performs an oscillatory behaviour with time. Maximum lift occurs once cavity is at maximum length while slight oscillation in the period oft=0.03-0.06 (for Kunz model) refers to small scale detachments stage of cloud cavitation. In this figure solution of Kunz model is closer to experimental data with less oscillatory peaks while Sauer model predicts higher peaks and hills for the lift. The averaged lift and drag coefficients over one cavitation cycle is given in Table 1 for both cavitation models and compared with the average data reported in Ref. [2]. As observed, the solution of Kunz model is quite close to the experimental data, with maximum of 3% error in average lift coefficient. However, both models over predict drag coefficient.

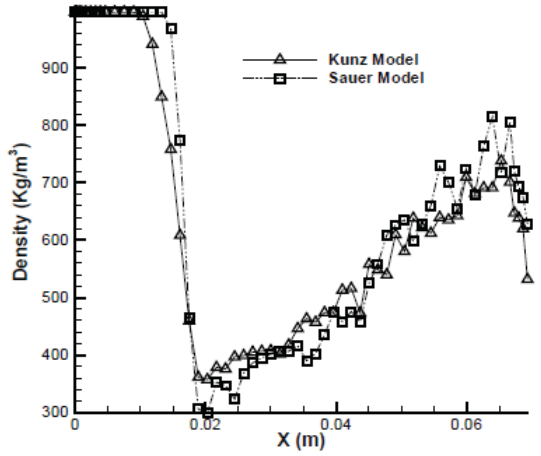

Figure 3: Average density distribution over the upper surface of the hydrofoil obtained from two cavitation models, namely Kunz model and Sauer model, σ=0.8.

Table 1: Averages of lift and drag coefficients.

	C_L	C_D
Sauer	0.70	0.140
Kunz	0.78	0.140
experiment	0.76	0.120

Figure 5 shows the temporal evolution of cloud cavitation over one cavitation cycle. These results correspond to LES turbulence model and both of Sauer and Kunz cavitation models. Results of Kunz model had shown for fewer time steps to avoid lengthy figure. The experimental pictures from Ref. [2] are also provided where available.

In cloud cavitation, the trailing edge becomes increasingly unsteady as bubbles are shed massively in the rear portion of the cavity. Additionally, cloud cavitation has a distinctly quasi-periodic pattern. Associated with the departing vertical flow, one observes substantial growth of the cavity thickness in the rear region of the cavity. As the re-entrant flow reaches the vicinity of leading edge of the cavity, the existing cavitating flow is pushed away from the wall, and a new cavitating flow structure forms there. The frames in Fig. 5 show the cavitation cycle as follows:

Frame (a-b): cavity grows while shedding occurs at the trailing edge,

Frame (c): cavity occupies most of the hydrofoil and is at its maximum extent. The peak observed in C_L diagram (Fig. 4) corresponds to this condition.

Frame (d): Breakdown and massive shedding occurs,

As expected, cloud cavitation regime is accompanied with cavity breakdown and vortex shedding. As Fig. 5 shows, there are good agreements between the current numerical solutions with those of experiments. This could be attributed to employing complex turbulence model, i.e., LES, in addition to benefiting from VOF technique in reconstructing the free surface as well as suitable cavitation models. However, Kunz and Sauer models differ in their cavity prediction. Sauer model predicts smaller detachments and stronger reentrant jet compared to the Kunz model. Stronger reentrant jet could results in smaller detachments.

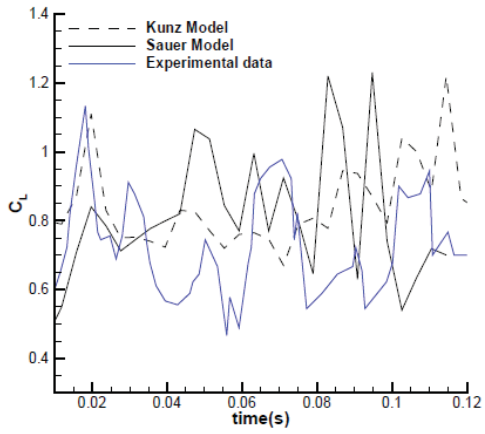

Figure 4: Variation of lift coefficient with time in cloud cavitation, current Kunz and Sauer models compared with the experimental data reported in Ref. [22].

4. Conclusion

In the present study a finite volume solver benefiting from the implicit LES turbulence model and accompanied with the VOF interface capturing method has been employed to capture unsteady cloud cavitation flow over the Clark-Y hydrofoil. The

simulation is performed under the framework of two phase flow solvers of OpenFOAM package. Effects of different mass transfer models including Kunz and Sauer models had been investigated. Our simulation shows that combination of the LES, VOF and Sauer or Kunz models has a suitable ability to simulate the shape of cloud cavitation and its dynamics with high accuracy. Also lift and drag coefficients as well as starting point of cavity are obtained close to the experimental data specially using the Kunz mass transfer model. It is also observed that Sauer model predicts smaller cavity detachments but stronger reentrant jet compared to the Kunz model.

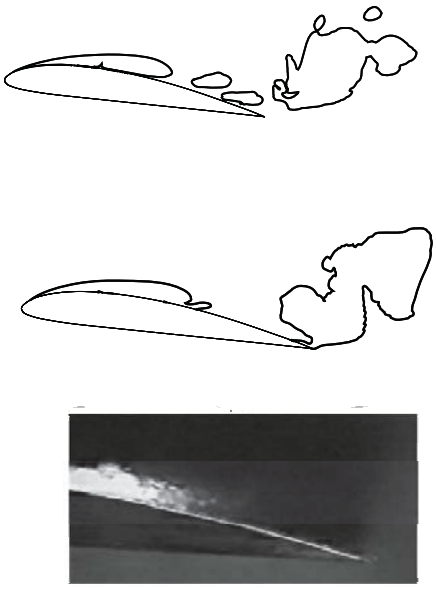

a)

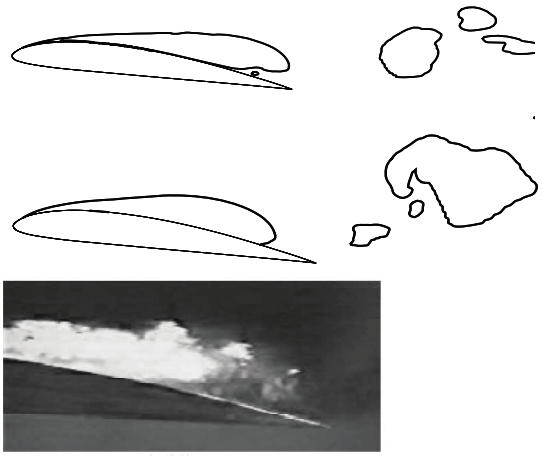

b)

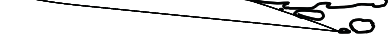

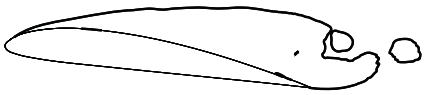

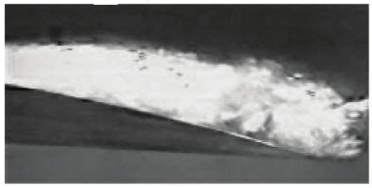

c)

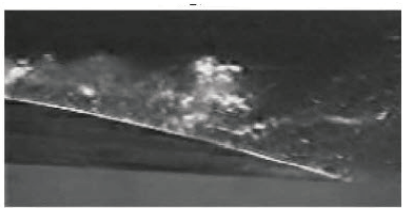

d)

Figure 5: Cavitation dynamics from the current simulation (with Kunz and Sauer models (top and middle pictures in each frame), σ=0.8. Experimental pictures (bottom) from Ref. [2].

REFERENCES

[1] Franc, J.P., Michel, J.M., 2004, Fundamentals of cavitation, Kluwer Academic Publisher, Netherlands.

[2] Wang, G., Senocak, I., Shyy, W., Ikohagi, T., Cao, S., 2001, Dynamics of attached turbulent cavitating flows, Prog. Aerosp. Sci. 37:551-581.

[3] Gopalan, S., Katz, J., 2000, Flow structure and modelling issues in the closure region of attached cavitation, Phys. Fluids 12, 895-911.

[4] Sauer J. 2000, Instationaren kaviterendeStromung - Ein neues Modell, baserend auf Front Capturing (VoF) and Blasendynamik, *PhD thesis,* Universitat, Karlsruhe.

[5] Yuan, W., Sauer, J., Schnerr, G.H., 2001, Modelling and computation of unsteady cavitation flows in injection nozzles, Journal of Mechanical Ind. 2, 383-394.

[6] Singhal, N. H., Athavale, A.K., Li, M., Jiang, Y., 2002, Mathematical basis and validation of the full cavitation model, J. of Fluids Eng., 124, 1-8.

[7] Merkle, C.L., Feng, J., Buelow, P.E.O., 1998, Computational Modelling of the Dynamics of Sheet Cavitation, Third International Symposium on Cavitation, (CAV1998), Grenoble, France.

[8] Kunz, R.F., Boger, D. A., Stinebring, D.R., Chyczewski, T.S., Lindau, J.W., Gibeling, H.J., 2000, A Preconditioned Navier-Stokes Method for Two-phase Flows with Application to Cavitation, Comput. Fluids 29, 849-875.

[9] Senocak I., shyy W. 2002, Evaluation of cavitation models for Navier-Stokes computations Proceeding of FEDSM 02, *ASME fluid engineering division summer meeting*, Montreal.

[10] Passandideh-Fard M., Roohi E., 2006, Coalescence collision of two droplets: bubble entrapment and the effects of important parameters, proceeding of the 14th Annual (International) Mechanical Engineering Conference, Isfahan, Iran.

[11] Noh W.F., Woodward P.R., 1976, SLIC Simple Line Interface Construction, Lecture Notes in Physics, Vol. 59, p. 330,.

[12] Hirt F.H., Nichols B.D. 1981, Volume of fluid (VOF) method for the dynamics of free boundaries, J. *Comput. Phys*. 39, 201.

[13] Youngs D.L. 1982, Time dependent multi material flow with large fluid distortion, *Num. Methods for Fluid Dynamics*, N.Y, 273-285.

[14] Ubbink O., 1999, Numerical prediction of two fluid systems with sharp interfaces, PhD thesis, Imperial College, University of London, UK.

[15] Ubbink O., Issa R.I., 1999, A method for capturing sharp fluid interfaces on arbitrary meshes, *Journal of Computational Physics*, 153, 26–50.

[16] Frobenius M., Schilling R.2003, Three-Dimensional unsteady cavitating effects on a single hydrofoil and in a radial pump- measurement and numerical simulation, Cav03-GS-9-005, Proceedings of the 5th international symposium on cavitation, Osaka.

[17] Wiesche S., 2005, Numerical simulation of cavitation effects behind obstacles and in an automotive fuel jet pumps, *Heat Mass Transfer*, 41,615-624.

[18] Bouziad A., Farhat M., Guennoun F., Miyagawa K.2003*, Physical modeling and simulation of leading edge cavitation, application to an industrial inducer,* Cav03-OS-6-014., Proceedings of the 5th international symposium on cavitation, Osaka, Japan.

[19] Wu J. Wang G., Shyy W., 2005, Time-dependent turbulent cavitating flow computations with interfacial transport and filter-based models, *Int. J. Numer. Meth. Fluids*, 49,739-761.

[20] Li D., Grekula M., Lindell P., 2009, A modified SST k-ε Turbulence Model to Predict the Steady and Unsteady Sheet Cavitation on 2D and 3D Hydrofoils*,* Proceedings of the 7th International Symposium on Cavitation CAV2009.

[21] Liu D., Hong F., Lu, F., 2010, The numerical and experimental research on unsteady cloud cavitating flow of 3D elliptical hydrofoil, *J. of Hydrodynamics*, 22, 759-763.

[22] Huang B., Wang G., 2011, Partially averaged Navier-Stokes method for time-dependent turbulent cavitating flows, *J. of Hydrodynamics*, 23, 26-33.

[23] Phoemsapthawee S., Leroux J., Kerampran S., Laurens J., 2012, Implementation of a transpiration velocity based cavitation model within a RANS solver*, European Journal of Mechanics B/Fluids* 32, 45–51.

[24] Wang G., Ostoja-Starzewski M., 2007, Large eddy simulation of a sheet/cloud cavitation on a NACA 0015 hydrofoil, Applied Mathematical Modeling, Vol. 31(3), 2007: 417-447.

[25] Huuva T., 2008, Large eddy simulation of cavitating and non-cavitating flow, PhD thesis, Chalmers University of Technology, Sweden.

[26] Liu D., Liu S., Wu Y. Xu H., 2009 , LES numerical simulation of cavitation bubble shedding on ALE 25 and ALE 15 hydrofoils, *J. of Hydrodynamics*, 21,807-813.

[27] Lu N., Bensow R. E., Bark G., 2010, LES of unsteady cavitation on the delft twisted foil, Journal of Hydrodynamics, Ser. B, Vol. 22 (5), 784-791.

[28] Passandideh-Fard M. Roohi E., 2008, Transient simulations of cavitating flows using a modified volume-of-fluid (VOF) technique, *International Journal of Computational Fluid Dynamics*, 22 , 97–114.

[29] Issa R. I. 1986, Solution of the implicitly discretized fluid flow equations by operator-splitting*, Journal of Computational Physics*, 62, 40–65.

[30] Bensow R. E., Bark G., 2010, Simulating cavitating flows with LES in OpenFOAM, 5th European Conference on Computational Fluid Dynamics, 2010.

[31] Sagaut P., 2006, Large Eddy Simulation for Incompressible Flows, *Springer, New York, 3rd* Edition.

[32] Bensow R. E. , Fureby C., 2007, On the Justification and Extension of Mixed Methods in LES, *Journal of Turbulence,* Vol.8, N54.

[33] Berberović E., van Hinsberg N.P., Jakirlić S., Roisman I.V., Tropea C., 2009, Drop impact onto a liquid layer of finite thickness: Dynamics of the cavity evolution, Physical Review E 79,036306.

[34] Berberović E., 2010, Investigation of Free-surface Flow Associated with Drop Impact: Numerical Simulations and Theoretical Modeling, Technische Universitat Darmstadt, Darmstadt.

[35] Weller H.G. A new approach to VOF-based interface capturing methods for incompressible and compressible flow*,* Technical Report TR/HGW/04, OpenCFD Ltd., 2008.

[36] Brackbill J.U., Kothe D.B., Zemach C., 1992, A continuum method for modelling surface tension, Journal of Computational Physics, 100,335–354.